Available online at www.sciencedirect.com
ScienceDirect
Trans. Nonferrous Met. Soc. China 27(2017) 1849−1855
Transactions of Nonferrous Metals Society of China
www.tnmsc.cn

Thermal decomposition kinetics of Algerian Tamazarte kaolinite by thermogravimetric analysis

D. REDAOUI[1], F. SAHNOUNE[2,3], M. HERAIZ[1], H. BELHOUCHET[1], M. FATMI[3]

1. Physics and Chemistry of Materials Laboratory, Department of Physics, University of M'sila, M'sila 28000, Algeria;
2. Department of Physics, University of M'sila, M'sila 28000, Algeria;
3. Research Unit on Emerging Materials (RUEM), University Ferhat Abbas of Setif 1, Setif 19000, Algeria

Received 30 June 2016; accepted 4 October 2016

Abstract: The decomposition kinetics of Algerian Tamazarte kaolinite (TK) was investigated using thermogravimetric analysis (TG). Differential thermal analysis (DTA) and TG experiments were carried out between room temperature and 1400 °C, at different heating rates from 10 to 40 °C/min. The activation energies, measured by DTG from isothermal treatments using Johnson−Mehl−Avrami (JMA) and Ligero methods and by non-isothermal treatments using Ozawa, Boswell and Kissinger methods, were around 151 and 144 kJ/mol, respectively. The Avrami parameter of growth morphology (indicating the crystallization mode) was found to be around 1.57 using non-isothermal treatments; however, when using isothermal treatments it is found to be equal to 1.35. The numerical factor, which depends on the dimensionality of crystal growth, is found to be 1.53 using Matusita equation. The frequency factor calculated by the isothermal treatment is equal to 1.55×10^7 s^{-1}. The results show that the bulk nucleation is followed by three-dimensional growth of metakaolinite with polyhedron-like morphology controlled by diffusion from a constant number of nuclei.

Key words: kaolinite; decomposition kinetics; Avrami parameter; activation energy; growth morphology

1 Introduction

Kaolin is widely used in a diverse applications in the industry of ceramics: conventional, structural and refractory ceramics, dielectrics and infrared transmitting materials [1,2]. Further than ceramics applications, kaolin also is utilized as an industrial filler agent for paper, rubber, plastics, cosmetics and paints [1,2]. Also, kaolin can be utilized for management of waste and preparation of geopolymers, geopolymer based composites and zeolites [1,3]. All these applications contain the thermal transformation of kaolinite and main mineral phase of kaolin. So, the course of metakaolinite development from kaolinite has been proved by some techniques and methods such as thermogravimetric analysis (TG), differential thermal analysis (DTA), differential scanning calorimetry (DSC) and dilatometry [2,3,4,5,6−14].

By using different factors such as the degree of structural ordering, adsorbed and substituted ions, shape and particle size, the thermal decomposition of kaolinite were determined. Also, the influence of instrumental conditions on the rate of decomposition is discussed in many works. In the range of temperature between 450 and 700 °C, the water release of kaolinite and the formation of the metakaolinite $Al_2Si_2O_7$ are well known. During the thermogravimetric investigation, the difference between the thermogravimetric mass loss (between 11.2% and 14.5% [4,5]) and the theoretical value of 13.95% is commonly reported.

In published works [6−16] the kinetics and mechanism of thermal decomposition of kaolinite and general clay mineral give large interesting. A full spectrum of methods, including molecular spectroscopy [6,7], electron microscopy [9] and thermal analysis techniques [8,10−12] were investigated in a massive process.

The aim of the present work is to study two corresponding processes during thermal decomposition of kaolin, such as dehydroxylation of kaolinite and the mechanism of dehydroxylation. The important kinetic parameters (overall activation energy and frequency factor) will be determined on the basis of TG experiments.

Corresponding author: M. FATMI; E-mail: fatmimessaoud@yahoo.fr
DOI: 10.1016/S1003-6326(17)60208-5

2 Experimental

Raw kaolin of Tamazarte (from Jijel, Algeria) was used in this investigation. Its chemical composition was determined by X-ray fluorescence (XRF) as shown in Table 1. The raw kaolin was milled by planetary ball with alumina grinding media for 4 h, after that it was milled by attrition for 2 h using ZrO_2 balls (diameter of 1.25 mm) at a speed of 700 rev/min. The slurry was dried at 150 °C, crushed manually then sieved through a 63 μm mesh.

Table 1 Chemical composition of raw kaolin (mass fraction, %)

Al_2O_3	SiO_2	Na_2O	P_2O_5	SO_3
33.00	61.73	0.14	0.03	0.03
K_2O	MgO	CaO	Fe_2O_3	
2.96	0.44	0.44	0.80	

Thermal analysis (DTA/TG) at the same time was carried out on a Setaram LABSYS Evo TG−DSC 1600 °C equipment, operated under Argon atmosphere. The samples were heated from room temperature up to 1400 °C at heating rates of 10 to 40 °C/min. The phases and their transformations were characterized by diffractometer system (XPERT-Pro) with a scan step of 0.0167° (Cu K_α radiation and a Ni filter) operated at 40 kV and 40 mA. The morphology of powders was characterized by a JEOL scanning electron microscope (SEM) model JMS 5600. The mechanism and kinetics of kaolinite transformation have been investigated by two different isothermal and non-isothermal methods. According to the information obtained about the thermal activities of kaolin, each technique gave excellent results.

Many methods have been introduced to calculate the activation energy (E_A) in the case of the non-isothermal method. In this study, just three of methods Ozawa [15,16], Boswell [17] and Kissinger were used [18−20]. The principle basics were listed by three formulas below:

$$\ln v = -1.0518\frac{E_A}{RT_p} + C_1 \quad (1)$$

$$\ln\frac{v}{T_p} = -\frac{E_A}{RT_p} + C_2 \quad (2)$$

$$\ln\frac{v}{T_p^2} = -\frac{E_A}{RT_p} + C_3 \quad (3)$$

where C_i (i=1, 2 and 3) is a constant, v is the heating rate in the DTG analysis, E_A is the activation energy, T_p is the absolute peak temperature in DTG curves, and R is the gas mole constant. The activation energy can be calculated by the slope obtained. The value of Avrami exponent, n, was determined from the shape of DTG curves at any heating rates as [21,22]

$$n = \frac{2.5T_p^2 R}{\Delta T_p E_A} \quad (4)$$

where ΔT_p is the width of crystallization peak at half maximum.

MATUSITA and SAKKA [23] have proposed a method to change Kissinger method as follows:

$$\ln\frac{v^n}{T_p^2} = C_3 - \frac{mE_A}{RT_p} \quad (5)$$

where m is a numerical factor which depends on the dimensionality of crystal growth and n is the Avrami parameter which indicates the crystallization mode.

Now in the second method (isothermal treatment of the TG/DTG obtained curves) the theoretical basis for interpreting TG results is determined by the Johnson−Mehl−Avrami (JMA) theory. Under an isothermal condition, the evolution of the crystallization fraction with the time (t) during a phase transformation can be described as

$$x=1-\exp[(-kt)^n] \quad (6)$$

where x is the volume fraction crystallized versus time (t), it was determined from the DTG results presented in the formula below:

$$x = \frac{A_T}{A_0} \quad (7)$$

where A_0 is the total area of the peak in the DTG curve between the temperature T_i (the initial of crystallization) and T_f (the completion of crystallization); A_T is the area under the peak between T_i and T; k is the reaction rate constant. Its temperature dependence is expressed by the Arrhenius type equation:

$$k = k_0\exp\left(-\frac{E_A}{RT}\right) \quad (8)$$

where k_0 is the frequency factor. Equations (6) and (8) lead to

$$\ln\left(\frac{dx}{dt}\right) = \ln(K_0 n) + \frac{n-1}{n}\ln[-\ln(1-x)] + \ln(1-x) - \frac{E_A}{RT}$$
$$= \ln[k_0 f(x)] - \frac{E_A}{RT} \quad (9)$$

LIGERO et al [24] suggested a mathematical method through non-isothermal techniques. The activation energy can be deduced from the slope of Eq. (9) if the authors select the same value of x in every experiment at different heating rates and plot for a given x. The function $\ln(dx/dt)$ versus $1/T$ shows that the plot of $\ln(dx/dt)$ versus $1/T$ at the same value of crystallized

fraction x at different heating rates. Hence, the Avrami parameter n was determined by the selection of many pairs of x_1 and x_2 that contain the condition $\ln[k_0 f(x_1)]=\ln[k_0 f(x_2)]$ for each heating rate, and using Eq. (9), the following equation is derived [24].

$$n=\frac{\ln[\ln(1-x_2)/\ln(1-x_1)]}{\ln\{(1-x_2)\ln(1-x_2)/[(1-x_1)\ln(1-x_1)]\}} \quad (10)$$

In addition, the frequency factor k_0 can be calculated by the following equation:

$$\ln[k_0 f(x_1)]=\ln k_0+\ln n+\frac{n-1}{n}[\ln(-\ln(1-x))]+\ln(1-x) \quad (11)$$

3 Results and discussion

Figure 1 shows the DTA/TG and DTG curves of kaolin powder heated from room temperature to 1400 °C at a heating rate of 30 °C/min. Two-step mass losses are observed on the TG curve. The first mass loss (Δm=1.5%) is due to the evaporation of adsorbed water and the formation of kaolinite. This transformation corresponds to the endothermic peak at 133 °C as seen in the DTA curve otherwise at 114 °C (first peak) in the DTG curve. The second step of mass loss (Δm=10%) is due to the dehydroxylation of kaolinite and the formation of metakaolinite, which corresponds to the endothermic peak at 582 °C seen in the DTA curve and corresponds to the second peak on the DTG curve at 580 °C. Two other exothermic peaks were observed on the DTA curve. The first one at 995 °C corresponds to the formation of primary mullite and amorphous silica SiO_2 and the second at 1198 °C corresponds to the amorphous transformation of SiO_2 to a crystalline phase (cristobalite). It is close to the value at 1200 °C reported by AZA et al [1] and PTÁČEK et al [25].

Figure 2 shows the XRD spectra of raw kaolin (Tamazarte) treated at different temperatures for 60 min. From ambient temperature to 200 °C, only reflections of aluminum silicate hydroxide ($Al_2Si_2O_5(OH)_4$ kaolinite) and silicon oxide (SiO_2, Quartz) were present. At 700 °C, complete transformation of kaolinite to metakaolinite was observed. A primary mullite phase starts to form from the spinel phase which was formed at 1000 °C. After this temperature, the transformation of the spinel phase to the primary mullite was completed and cristobalite started to form through the transformation of silica and quartz at 1200 °C. All the transformations of kaolin in DTA/DTG results are confirmed by the XRD phase analysis as shown in Fig. 2.

Figure 3 shows the scanning electron micrographs of kaolin powder before milling and after milling (in planetary ball for 4 h and then milled by attrition for 2 h). It can be clearly seen that the powder of kaolin has a large particle size distribution and an irregular shape. However, milling decreased the particle size, and yielded a homogeneous powder mixture with particles having almost spherical shape. These parameters (small particle size and spherical shape) play an important effect in the sintering and compaction of the powder through reduction of time and temperature sintering.

Figure 4 shows the variation of the crystallized fraction of metakaolinite (dehydroxylated of kaolinite) which was calculated using Eq. (7) from TG experiments and the differential thermogravimetry (DTG). It can be seen that the temperature of the maximum rate of dehydroxylation curves peak position (T_p) is shifted to a higher temperature from 537 to 588 °C when the heating rate increased from 10 to 40 °C/min. The increase of heating rate shifts the rate of the variation of the crystallized fraction from 0.146 to 0.623 min^{-1} and the time of the crystallized fraction decreases from 12.5 to 3 min.

Figure 5 presents the derivation of relative mass loss change analysis curves for Tamazarte kaolinite at

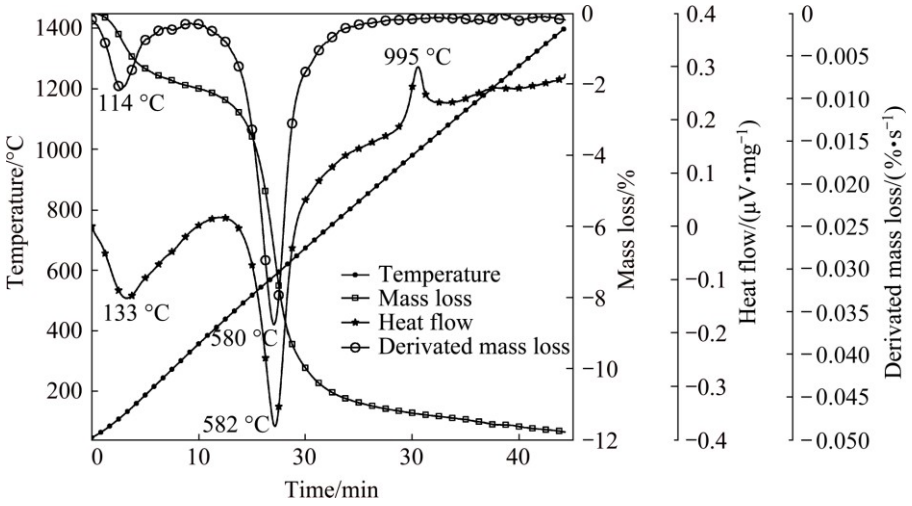

Fig. 1 DTA/TG and DTG curves of Tamazarte kaolin powder heated at 30 °C/min

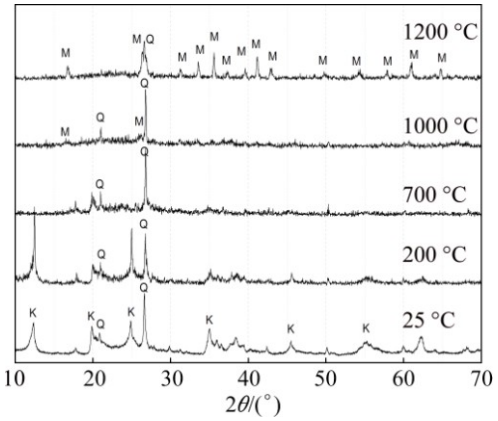

Fig. 2 XRD patterns of raw kaolin treated at different temperatures

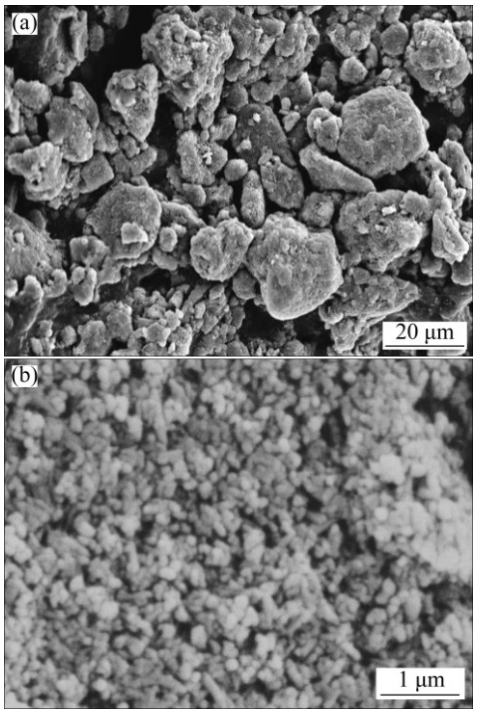

Fig. 3 SEM images of raw kaolin powder (a) and kaolin powder (b) after milling (in planetary ball for 4 h and by attrition for 2 h)

different heating rates between 400 and 700 °C and the plots according to Kissinger (Eq. (3)), Ozawa (Eq. (1)) and Boswell (Eq. (2)) methods. The activation energies of dehydroxylated kaolinite calculated from the slope of the function $Y_i=f(1/T_p)$ are listed in Table 2. The average of activation energy is 144 kJ/mol. The above values of activation energy fall in the range 115−250 kJ/mol [1,3,13,26−29] (115, 227, 119, 178, 188, 197 and 248 kJ/mol, respectively). The difference between the reported values of activation energy of dehydroxylated kaolinite was attributed to many factors such as kaolinite structure [6], heating rate [30] and impurities [27]. Table 3 presents the values of the Avrami parameters which indicate the crystallization mode, n, for different heating rates using Eq. (4). The average Avrami parameter is 1.55, which suggests that the crystallization process of meta kaolinite should be controlled by a diffusion growth [31].

Figure 6 shows the plots of $\ln(v^n/T_p^2)$ versus $1/T_p$ according to Matusita equation (Eq. (5)). The dimensionality of crystal growth, m, calculated from the slope of the function $\ln(v^n/T_p^2)=f(1/T_p)$, is found to be

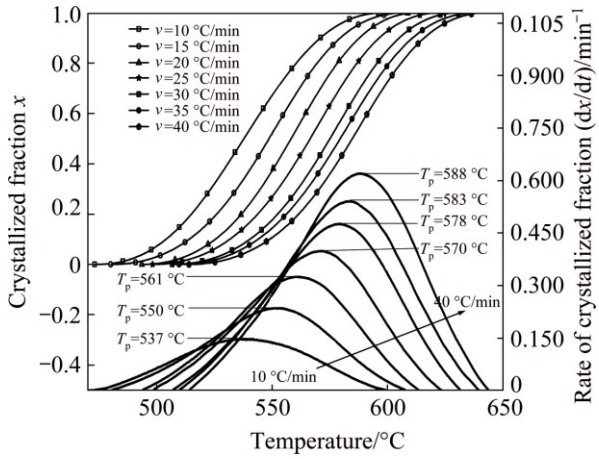

Fig. 4 Crystallized fractions and rate of crystallized fraction of metakaolinite formation at different heating rates

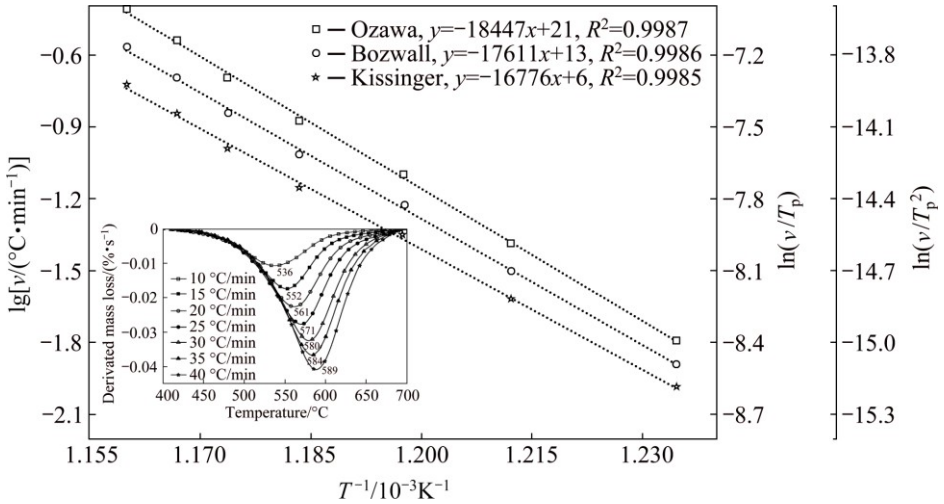

Fig. 5 Corresponding plots of dehydroxylation of kaolinite at different heating rates

Table 2 Values of E_A and R^2 for kaolinite dehydroxylation by using Ozawa, Boswell and Kissinger methods from TG/DTG experiments

Method	E_A/(kJ·mol^{-1})	R^2
Ozawa	146	0.9987
Boswell	146	0.9986
Kissinger	140	0.9985

Table 3 Values of Avrami parameter n for different heating rates from TG/DTG experiments

v/(°C·min^{-1})	ΔT	T_p/°C	n
10	67.14	536.64	1.4
15	63.81	550.54	1.51
20	62.088	560.67	1.59
25	62.85	570.86	1.61
30	63.51	578.03	1.62
35	65.04	582.63	1.60
40	64.89	587.85	1.62

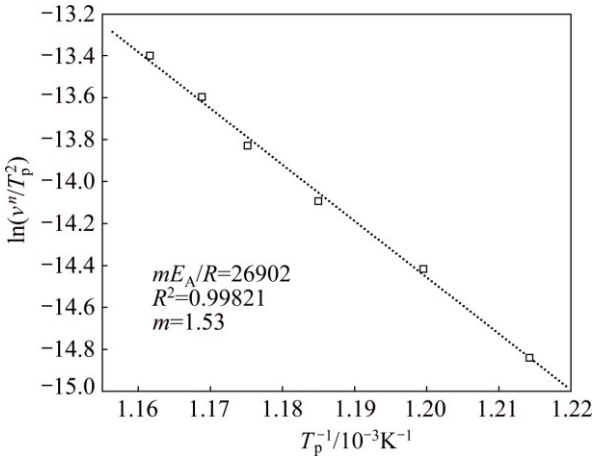

Fig. 6 Plot of $\ln(v^n/T^2_p)$ versus $1/T_p$ according to Matusita equation

1.53 for the dehydroxylated of kaolinite. Both growth morphology parameters n and m are close to 1.5. These results also indicate that bulk nucleation is followed by three-dimensional growth of metakaolinite with polyhedron-like morphology controlled by diffusion from a constant number of nuclei.

Figure 7 presents the plot of $\ln(dx/dt)$ and $1/T$ versus crystallized fraction x at different heating rates from TG/DTG experiment. A mathematical method through non-isothermal techniques was proposed by LIGERO et al [24]. If the same value of crystallized fraction x in every experiment at different heating rates is selected, the function $\ln(dx/dt)$ versus $1/T$ gives a linear curve (Fig. 8). The activation energy can be calculated from the slope of the function $\ln(dx/dt)=f(1/T)$ [24,32]. The values of activation energy E_A for different crystallized fractions, which are calculated by the average of the slopes of the lines, are listed in Table 4. The coefficient of determination R^2 is greater than 0.99 for different x values. The average activation energy of dehydroxylated kaolinite is 151 kJ/mol, which is in good agreement with that of 144 kJ/mol estimated by non-isothermal TG/DTG treatment.

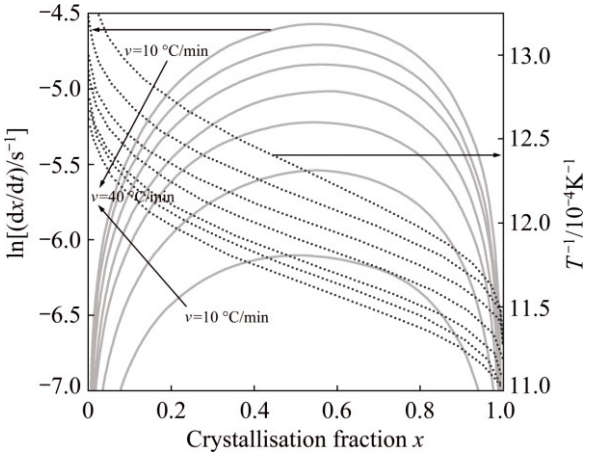

Fig. 7 Plot of $\ln(dx/dt)$ and $1/T$ versus of crystallized fraction x at different heating rates

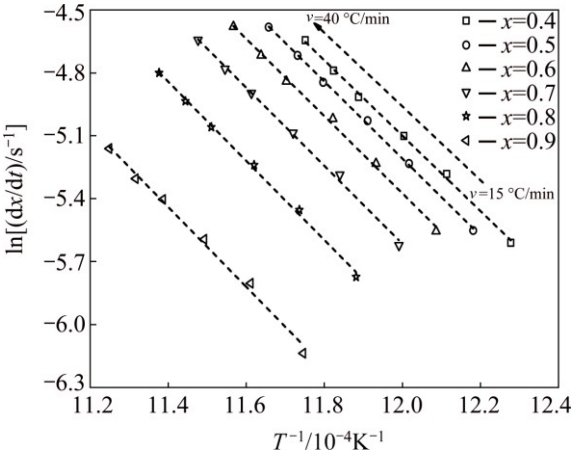

Fig. 8 Plots of $\ln(dx/dt)$ versus $1/T$ at same value of crystallized fraction x at different heating rates

Table 4 Activation energy E_A and coefficient of determination R^2 for different crystallized fractions

x	R^2	E_A/(kJ·mol^{-1})
0.1	0.998	147
0.2	0.994	145
0.3	0.995	146
0.4	0.997	149
0.5	0.998	152
0.6	0.996	153
0.7	0.996	154
0.8	0.997	156
0.9	0.992	158

Figure 9 presents the plot of $\ln[k_0 f(x)]$ versus crystallization fraction x at different heating rates (20, 30 and 40 °C/min). The Avrami parameter, n, was determined by the selection of many pairs of x_1 and x_2 that satisfied the condition $\ln[k_0 f(x_1)]=\ln[k_0 f(x_2)]$ using Eq. (10). The average values of Avrami parameter, n, for each heating rate are listed in Table 5. The average Avrami parameter is 1.35. The frequency factor, k_0, can be calculated by Eq. (11); the average value of k_0 is 1.55×10^7 s^{-1}.

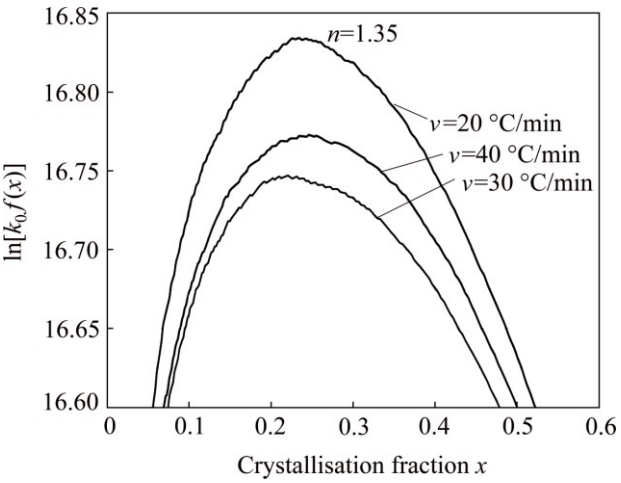

Fig. 9 Plots of $\ln[k_0 f(x)]$ versus crystallization fraction for kaolin powder heated at different heating rates

Table 5 Values of Avrami parameter, $t_{0.75}/t_{0.25}$ value and frequency factor at different heating rates

v/(°C·min^{-1})	n	$t_{0.75}/t_{0.25}$	$k_0/10^7$
10	1.30	1.61	1.99
15	1.34	1.66	1.50
20	1.36	1.70	1.61
25	1.35	1.70	1.58
30	1.36	1.69	1.52
35	1.34	1.70	1.55
40	1.38	1.69	1.56

n_{moy}=1.35; $(t_{0.75}/t_{0.25})_{moy}$=1.67; $(k_0)_{moy}=1.55\times10^7$

From the ratio of time for two fixed degrees of transformation, the morphology of the crystal growth can be obtained [31,32]. A suitable representative index is the ratio of time for 75% and 25% transformation, in such a way we find $1.48\leq t_{0.75}/t_{0.25}\leq1.69$ for 3D growth (polyhedron), $1.69\leq t_{0.75}/t_{0.25}\leq2.20$ for two-dimensional growth (plates) and $2.20\leq t_{0.75}/t_{0.25}\leq4.82$ for one-dimensional growth (needles). The average values of $t_{0.75}/t_{0.25}$ for each heating rate are listed in Table 5. For all the heating rates the average value is 1.67. This suggests a three-dimensional growth of metakaolinite crystals [32].

4 Conclusions

1) The activation energies, measured by DTG from isothermal and non-isothermal treatments were around 151 and 144 kJ/mol, respectively.

2) The Avrami parameters of growth morphology were found to be around 1.57 and 1.35 using non-isothermal and isothermal treatments, respectively.

3) The numerical factor, which depends on the dimensionality of crystal growth, is found to be 1.53 using Matusita equation.

4) The frequency factor calculated by the isothermal treatment is 1.55×10^7 s^{-1}.

5) The bulk nucleation is dominant in metakaolinite formation followed by three-dimensional growth of metakaolinite with polyhedron-like morphology controlled by diffusion from a constant number of nuclei.

References

[1] de AZA A H, TURRILLAS X, RODRIGUEZ M A, DURAN T, PENA P. Time-resolved powder neutron diffraction study of the phase transformation sequence of kaolinite to mullite [J]. Journal of the European Ceramic Society, 2014, 34: 1409−1421.

[2] FRANCO F, PÉREZ-MAQUEDA L A, PÉREZ-RODRÍGUEZ J L. The effect of ultrasound on the particle size and structural disorder of a well-ordered kaolinite [J]. Journal of Colloid and Interface Science, 2004, 274: 107−117.

[3] PTÁČEK P, ŠOUKAL F, OPRAVIL T, HAVLICA J, BRANDŠTETR J. The kinetic analysis of the thermal decomposition of kaolinite by DTG technique [J]. Powder Technology, 2011, 208: 20−25.

[4] SAHNOUNE F, SAHEB N, KHAMEL B, TAKKOUK Z. Thermal analysis of dehydroxylation of Algerian kaolinite [J]. Journal of Thermal Analysis and Calorimetry, 2012, 107: 1067−1072.

[5] SAHNOUNE F, CHEGAAR M, SAHEB N, GOEURIOT P, VALDIVIESO F. Algerian kaolinite used for mullite formation [J]. Applied Clay Science, 2008, 38: 304−310.

[6] HEIDE K, FÖLDVARI M. High temperature mass spectrometric gas-release studies of kaolinite $Al_2[Si_2O_5(OH)_4]$ decomposition [J]. Thermochimica Acta, 2006, 446: 106−112.

[7] TEMUUJIN J, OKADA K, MACKENZIE K J D, JADAMBAA T S. The effect of water vapour atmospheres on the thermal transformation of kaolinite investigated by XRD, FTIR and solid state MAS NMR [J]. Journal of the European Ceramic Society, 1999, 19: 105−112.

[8] PÉREZ-RODRÍGUEZ J L, PASCUAL J, FRANCO F, JIMÉNEZ DE HARO M C, DURAN A, RAMÍREZDEL VALLE V, PÉREZ-MAQUEDA L A. The influence of ultrasound on the thermal behavior of clay minerals [J]. Journal of the European Ceramic Society, 2006, 26: 747−753.

[9] de SOUZA SANTOS H, CAMPOS T W, DE SOUZA SANTOS P, KIYOHARA P K. Thermal phase sequences in gibbsite/kaolinite clay: Electron microscopy studies [J]. Ceramics International, 2005, 31: 1077−1084.

[10] TRAORÉ K, GRIDI-BENNADJI F, BLANCHART P. Significance of kinetic theories on the recrystallization of kaolinite [J]. Thermochimica Acta, 2006, 451: 99−104.

[11] BALEK V, MURAT M. The emanation thermal analysis of kaolinite clay minerals [J]. Thermochimica Acta, 1996, 282: 385−397.

[12] LIU Ya-fei, LIU Xing-qin, TAO Shan-wen, MENG Guang-yao, SORENSEN O T. Kinetics of the reactive sintering of kaolinite–aluminum hydroxide extrudate [J]. Ceramics International, 2002, 28: 479−486.
[13] SAIKIA N, SENGUPTA P, GOGOI P K, BORTHAKUR P C H. Kinetics of dehydroxylation of kaolin in presence of oil field effluent treatment plant sludge [J]. Applied Clay Science, 2002, 22: 93−102.
[14] LEVY J H, HURST H J. Kinetics of dehydroxylation, in nitrogen and water vapour, of kaolinite and smectite from Australian Tertiary oil shales [J]. The Science and Technology of Fuel and Energy, 1993, 72: 873−877.
[15] OZAWA T. A new method for analyzing thermogravimetric data [J]. Bulletin of the Chemical Society of Japan, 1965, 38: 1881−1886.
[16] FLYNN J H, WALL L A. General treatment of the thermogravimetry of polymers [J]. Journal of Research of the National Bureau of Standards A: Physics and Chemistry, 1966, 70A: 487−523.
[17] BOSWELL P G. On the calculation of activation energies using modified Kissinger method [J]. Journal of Thermal Analysis, 1980, 18: 353–58.
[18] KISSINGER H E. Reaction kinetics in differential thermal analysis [J]. Analytical Chemistry, 1957, 29: 1702−1706.
[19] ZHAN Guang, YU Jun-xia, XU Zhi-gao, CHI Ru-an. Kinetics of thermal decomposition of lanthanum oxalate hydrate [J]. Transactions of Nonferrous Metals Society of China, 2012, 22: 925–934.
[20] COATS A W, REDFERN J P. Kinetic parameters from thermogravimetric data [J]. Letters Nature, 1964, 201: 68−69.
[21] RAY C S, HUANG W, DAY D E. Crystallization kinetics of a lithia silica glass: Effect of sample characteristics and thermal-analysis measurement techniques [J]. Journal of the American Ceramic Society, 1991, 74: 60−66.
[22] AUGIS J A, BENNET J E. Calculation of Avrami parameters for heterogeneous solid-state reactions using a modification of Kissinger method [J]. Journal of Thermal Analysis, 1978,13: 283−292.
[23] MATUSITA K, SAKKA S. Kinetic study of crystallization of glass by differential thermal analysis-criterion on application of Kissinger plot [J]. Journal of Non-Crystalline Solids, 1980, 39: 741−746.
[24] LIGERO R A, VAZQUES J, VILLARES P, JIMENEZ-GARAY R. A study of the crystallization kinetics of some Cu−As−Te glasses [J]. Journal of Materials Science, 1991, 26: 211−215.
[25] PTÁČEK P, KŘEČKOVÁ M, ŠOUKAL F, OPRAVIL T, HAVLICA J, BRANDŠTETR J. The kinetics and mechanism of kaolin powder sintering I: The dilatometric CRH study of sinter-crystallization of mullite and cristobalite [J]. Powder Technology, 2012, 232: 24−30.
[26] PTÁČEK P, KUBÁTOVÁ D, HAVLICA J, BRANDŠTETR J, ŠOUKAL F, OPRAVIL T. The non-isothermal kinetic analysis of the thermal decomposition of kaolinite by thermogravimetric analysis [J]. Powder Technology, 2010, 204: 222−227.
[27] PRODANOĆ D, ŽIVKOVIĆ Ž D, DUMIĆ M. The kinetics of dehydroxylation and mullitization of zettlitz kaolin in the presence of calcium (II) as an ingredient [J]. Thermochimica Acta, 1989, 156: 61−67.
[28] NAHDI K, LLEWELLYN P, ROUQUÉROL F, ROUQUÉROL J, ARIGUIB N K, AYEDI M T. Controlled rate thermal analysis of kaolinite dehydroxylation: Effect of water vapour pressure on the mechanism [J]. Thermochimica Acta, 2002, 390: 123−132.
[29] PTÁČEK P, ŠOUKAL F, OPRAVIL T, NOSKOVÁ M, HAVLICA J, BRANDŠTETR J. The non isothermal kinetics analysis of the thermal decomposition of kaolinite by effluent gas analysis technique [J]. Powder Technology, 2010, 203: 272−276.
[30] CASTELEIN O, SOULESTIN B, BONNET J P, BLANCHART P. The influence of heating rate on the thermal behaviour and mullite formation from a kaolin raw material [J]. Ceramics International, 2001, 27: 517−522.
[31] MATUSITA K, MIURA K, KOMATSU T. Kinetics of no-isothermal crystallization of some fluoro zirconate glasses [J]. Thermochim. Acta, 1985, 88: 283−288.
[32] ROMERO M, MARTI´N-MA´RQUEZ J, RINCO´N J M A. Kinetic of mullite formation from a porcelain stoneware body for tiles production [J]. Journal of the European Ceramic Society, 2006, 26: 1647−1652.

用热重分析法研究阿尔及利亚 Tamazarte 高岭土的热分解动力学

D. REDAOUI[1], F. SAHNOUNE[2,3], M. HERAIZ[1], H. BELHOUCHET[1], M. FATMI[3]

1. Physics and Chemistry of Materials Laboratory, Department of Physics, University of M'sila, M'sila 28000, Algeria;
2. Department of Physics, University of M'sila, M'sila 28000, Algeria;
3. Research Unit on Emerging Materials (RUEM), University Ferhat Abbas of Setif 1, Setif 19000, Algeria

摘　要：采用热重分析法(TG)和研究阿尔及利亚 Tamazarte 高岭土的热分解动力学。差热分析(DTA)和 TG 实验在室温~1400 ℃ 下进行，加热速率为 10~40 ℃/min。采用 JMA 和 Ligero 法由等温处理测得的活化能，以及采用 OFW 和 KAS 法由非等温处理测得的活化能，分别约为 151 和 144 kJ/mol。采用非等温处理确定的生长形貌 Avrami 参数约为 1.57，而采用等温处理时该值约为 1.35。数值因数与晶体生长的维度有关，采用 Matusita 方程确定的值为 1.53。采用等温处理时，计算得到的频率因子为 1.55×10^7 s^{-1}。结果表明，块体形核之后伴随偏高岭土的三维生长，偏高岭土具有受扩散控制的多面体结构，以一定数量的晶核开始生长。

关键词：高岭土；分解动力学；Avrami 参数；活化能；生长形貌

(Edited by Xiang-qun LI)